

Benzoyl Radical Decomposition Kinetics: Formation of Benzaldehyde + H, Phenyl + CH₂O, and Benzene + HCO

Gabriel da Silva^{*,†} and Joseph W. Bozzelli^{*,‡}

Department of Chemical and Biomolecular Engineering, The University of Melbourne, Victoria 3010, Australia, and Department of Chemistry and Environmental Science, New Jersey Institute of Technology, Newark, New Jersey 07102

Received: March 19, 2009; Revised Manuscript Received: May 21, 2009

The kinetics of benzoyl radical decomposition was studied using ab initio computational chemistry and RRKM rate theory. The benzoyl radical is an important but short-lived intermediate in the combustion of toluene and other alkylated aromatic hydrocarbons. A theoretical study of the thermochemistry and kinetics to products over a range of temperatures and pressures for benzoyl decomposition is reported. Ab initio calculations with the G3X theoretical method reveal low-energy pathways from the benzoyl radical to benzaldehyde + H and the phenyl radical + formaldehyde (CH₂O), as well as a novel mechanism to benzene + the formyl radical (HC[•]O). RRKM simulations were performed for benzoyl decomposition as a function of temperature and pressure. Benzaldehyde formation constitutes more than 80% of the total reaction products at temperatures below 1000 K, decreasing to around 50% at 2000 K. Formation of benzene + HC[•]O and phenyl + CH₂O is of similar importance, each accounting for 5–10% of the decomposition products at around 1000 K, increasing to 20–30% at 2000 K. The results presented here should lead to improved kinetic models for the oxidation of alkylated aromatic hydrocarbons, particularly for the formation of benzene as a direct oxidation product of toluene. Re-evaluation of the phenyl radical heat of formation leads us to suggest a benzene C–H bond dissociation energy in the range of 113.5–114.5 kcal mol⁻¹.

Introduction

Aromatic hydrocarbons are one of the major components of liquid fuels such as gasoline and jet fuel, as they provide high energy per volume as well as good antiknock characteristics (high octane rating). Benzene, a suspected carcinogen, is currently being eliminated as a component of transportation fuels. Consequently, alkylated aromatics such as toluene, ethylbenzene, and the xylenes are finding increased use. Accordingly, there is a great deal of interest in modeling the oxidation kinetics of toluene and other alkylated aromatics. Despite this interest, many key reaction processes in the toluene oxidation mechanism have not been extensively studied, and we do not have a detailed understanding of how alkyl substituents affect the autoignition and oxidation of aromatics.¹ Furthermore, existing models for oxidation of toluene and the xylenes fail to adequately reproduce certain experimental results (ignition delays, species profiles), especially under autoignition conditions of high pressure and low temperature. As such, recent attention has turned to the development of detailed kinetic models for the oxidation of substituted aromatics, and aromatic fuel blends, that are applicable over wide pressure and temperature ranges.^{2–6}

The oxidation of toluene primarily results in formation of the benzyl radical as the initial reaction intermediate, through abstraction of a weak methyl hydrogen atom (bond dissociation energy (BDE) = 91.7 kcal mol⁻¹).⁷ The benzyl radical is resonantly stabilized and is not rapidly oxidized by molecular oxygen. Instead, it reacts slowly to produce benzaldehyde +

OH, or the benzylperoxy radical at low temperatures and high pressures.⁸ The benzyl radical also rapidly recombines with free H atoms to return toluene. As a result, abstraction of the higher energy ring H atoms⁹ (BDE = 112.9 kcal mol⁻¹)⁷ and homolytic fission of the C–C bond¹⁰ (BDE = 103.6 kcal mol⁻¹)⁷ are also important. These reactions produce respective methylphenyl and phenyl radicals, which react rapidly with O₂ to produce a variety of new unsaturated (oxy)-hydrocarbon products.^{11–15}

The resonantly stabilized benzyl radical will readily react with a range of common combustion intermediates, including the hydroxyl (OH)¹⁶ and hydroperoxyl (HO₂)^{16,17} radicals, and atomic oxygen (O(³P)).^{18,19} Such reactions are expected to be of importance following establishment of the radical pool. The benzyl + HO₂ reaction forms the benzoyl radical (C₆H₅CH₂O), with rate constant of around 10¹³ cm³ mol⁻¹ s⁻¹ at temperatures of ca. 800 K and above. At temperatures below 800 K, quenching of the benzylhydroperoxide adduct becomes an important process. Benzylhydroperoxide can also form by H addition and abstraction reactions in the benzylperoxy radical and has been proposed as the key species in liquid-phase toluene oxidation.²⁰ Benzylhydroperoxide decomposes to benzoyl + OH with a barrier of only 45.0 kcal mol⁻¹,¹⁷ making this reaction rapid at even moderate temperatures. Another potential pathway to the benzoyl radical in aromatic oxidation is via the reaction of benzyl radicals with atomic oxygen. While the activated C₇H₇O adduct formed in the benzyl + O association is expected to rapidly dissociate to new products, the formation of stabilized benzoyl radicals may be important, especially under autoignition conditions.

It is clear that the benzoyl radical is an important intermediate in the oxidation of toluene and other substituted aromatic hydrocarbons. The benzoyl radical is expected to promptly decompose to new products, but thermal decomposition of the

* To whom correspondence should be addressed. E-mail: gdasilva@unimelb.edu.au; bozzelli@njit.edu.

[†] University of Melbourne.

[‡] New Jersey Institute of Technology.

benzoyl radical is not well characterized with respect to either the decomposition products or kinetics. Earlier models for toluene oxidation generally assume that the benzoyl radical decomposes solely to benzaldehyde + H,²¹ although some more recent studies have included pathways to phenyl + CH₂O.^{2,4,6} A molecular dynamics simulation of the *o*-xylene/O₂ oxidation reaction at 2500 K predicted formation of the *o*-methylbenzoyl radical via the *o*-methylbenzyl + HO₂ reaction, followed by decomposition to the *o*-methylphenyl radical + CH₂O.²² Treatment of benzoyl radical decomposition in current kinetic models is reviewed in further detail later in this article, although it is clear that this treatment is at present inconsistent.

In this study, we investigate the thermal decomposition of the benzoyl radical, using first principles computational chemistry and RRKM rate theory. Our aim is to accurately characterize the kinetics and product branching ratios of benzoyl radical decomposition over a wide range of temperature and pressure conditions, in an effort to improve kinetic models for aromatic hydrocarbon oxidation.

Methods

All located minima and transition states on the C₇H₇O potential energy surface were studied with the B3LYP/6-31G(2df,p) DFT method for geometries and vibrational frequencies. The high-level G3X composite theoretical method was used for molecular energies.²³ Standard heats of formation ($\Delta_f H^\circ_{298}$) were calculated for all species at the G3X level using atomization work reactions, with 298 K reference enthalpies of 171.29, 59.567, and 52.103 kcal mol⁻¹ for the C, O, and H atoms, respectively.²⁴ All calculations were performed using Gaussian 03.²⁵ Geometries (in Cartesian coordinates, Å), energies (in hartrees), vibrational frequencies, and moments of inertia are available in the Supporting Information.

The G3X method was selected here for its ability to provide accurate thermochemical and kinetic properties at reasonable computational cost for moderate-sized molecules. G3X calculations reproduce the experimental energies of the G3/99 test with a mean average deviation of 0.95 kcal mol⁻¹, or 0.56 and 0.76 kcal mol⁻¹ for the respective substituted hydrocarbon and radical subsets.²³ The G3 class of methods also performs well for barrier heights, which are required to accurately calculate rate constants (the similar G3SX method reproduces barrier heights of the DBH24/08 test set with a mean unsigned error of 0.57 kcal mol⁻¹).²⁶ In this study, we estimate 95% confidence limit uncertainties in the reaction enthalpies and barrier heights of 1.5 kcal mol⁻¹. Uncertainties in the atomization heats of formation may be larger, due to a lesser degree of error cancellation across the atomization work reactions.

Thermochemical properties, including $\Delta_f H^\circ$ and S° , were evaluated from 300 to 2000 K according to statistical mechanical principles in ChemRate version 1.5.2.²⁷ Low-frequency vibrational modes were treated as hindered internal rotors, using B3LYP/6-31G(d) level rotor potentials (Supporting Information). High-pressure limit rate constants (k^∞) for elementary reactions were also obtained in ChemRate, from the application of canonical transition state theory. Reactions that predominantly involved movement of a H atom were corrected for quantum mechanical tunnelling using the Eckart formalism.²⁸ Rate constants between 300 and 2000 K were fit to the three-parameter Arrhenius equation $k^\infty = A'T^n \exp(-E_a/RT)$ to obtain the rate parameters A' , n , and E_a .

Apparent rate constants were evaluated from 300 to 2000 K and 0.01 to 100 atm using RRKM theory for $k(E)$ with master equation analysis for pressure falloff, in the ChemRate program.

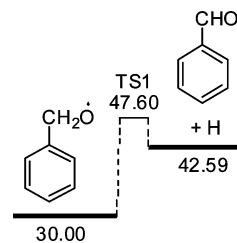


Figure 1. Decomposition of benzoyl to benzaldehyde + H via direct C–H bond dissociation.

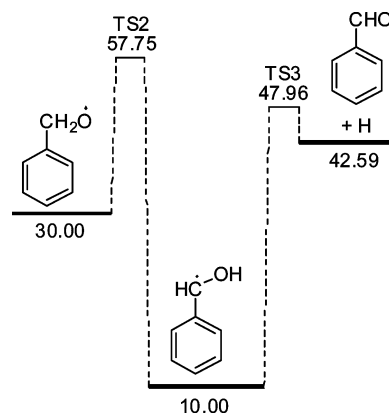


Figure 2. Decomposition of benzoyl to benzaldehyde + H via rearrangement to the α -hydroxybenzyl radical.

Collisional energy transfer was described using an exponential down model, with $\langle \Delta E_{\text{down}} \rangle = 2000 \text{ cm}^{-1}$.^{7,29} Lennard-Jones collision parameters for the C₇H₇O species were $\sigma = 6.5 \text{ Å}$ and $\epsilon/k = 550 \text{ K}$. N₂ was used as the buffer gas.

Results and Discussion

Mechanism and Energy Diagrams. We consider unimolecular decomposition of the benzoyl radical to benzaldehyde + H, benzene + HC[•]O, and phenyl + CH₂O via several different pathways. Enthalpy diagrams (G3X $\Delta_f H^\circ_{298}$) for each of the considered reaction processes are depicted in Figures 1–6. All of these reaction mechanisms are relatively low energy (barrier heights below 40 kcal mol⁻¹), and as such benzoyl decomposition is expected to be rapid at even moderate temperatures.

Three pathways are considered for the formation of benzaldehyde + H. First, benzaldehyde can form via simple C–H bond scission in the benzoyl radical (the “direct” mechanism, Figure 1). This reaction proceeds with a barrier of only 17.6 kcal mol⁻¹ and is endothermic by only 12.6 kcal mol⁻¹. Overall, this is the lowest energy decomposition reaction considered in this study and is expected to be dominant at lower temperatures. This is a β -scission elimination reaction, and we expect a moderate pre-exponential factor (small change in entropy). Figures 2 and 3 illustrate two multistep mechanisms for benzaldehyde + H formation (the respective “indirect I” and “indirect II” mechanisms). In these mechanisms, benzoyl first rearranges to another C₇H₇O isomer via an intramolecular hydrogen shift. Isomerization to the considerably more-stable α -hydroxybenzyl radical takes place with a barrier of ca. 28 kcal mol⁻¹ (TS2); the α -hydroxybenzyl radical can then undergo O–H dissociation to form benzaldehyde + H (TS3), with a barrier of 37.8 kcal mol⁻¹ or 18.0 kcal mol⁻¹ above the benzoyl radical. The relatively high-energy transition state for the initial rearrangement to α -hydroxybenzyl makes it unlikely that this process is important in benzoyl decomposition, although tunnelling will increase the rate of the initial hydrogen shift

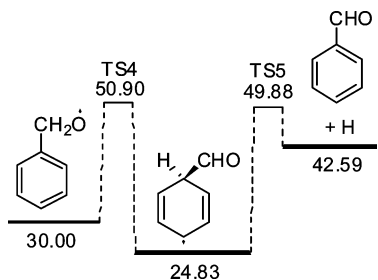


Figure 3. Decomposition of benzoxyl to benzaldehyde + H via rearrangement to the 2,5-cyclohexadien-4-formyl-1-yl radical.

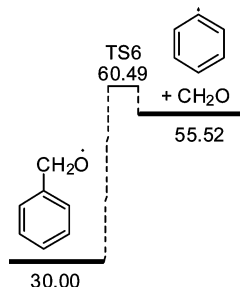


Figure 4. Decomposition of benzoxyl to phenyl + CH₂O via direct C–C bond dissociation.

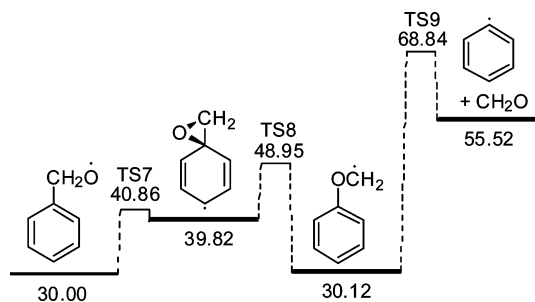


Figure 5. Decomposition of benzoxyl to phenyl + CH₂O via rearrangement to the phenoxymethyl radical.

reaction at lower temperatures. Additionally, decomposition of the α -hydroxybenzyl radical to benzaldehyde + H may be of significance in other reaction mechanisms, where this radical is formed directly.³ Isomerization of benzoxyl to the 2,5-cyclohexadien-4-formyl-1-yl radical is a lower-energy process, requiring only 21 kcal mol⁻¹ (TS4). Further decomposition to benzaldehyde + H is energetically competitive with the reverse reaction to benzaldehyde + H (TS5), although as we show later 2,5-cyclohexadien-4-formyl-1-yl prefers to undergo C–C scission to benzene + HC[•]O.

Two reaction pathways are considered for phenyl + CH₂O formation from benzoxyl. Again, benzoxyl can decompose directly to these products via C–C β -scission (Figure 4). This reaction requires an energy barrier of 30.5 kcal mol⁻¹ (TS6) and is endothermic by 25.5 kcal mol⁻¹. Decomposition of the benzoxyl radical to phenyl + CH₂O is a somewhat higher-energy process than the direct benzaldehyde + H decomposition reaction or the intramolecular hydrogen shifts considered above. This C–C bond dissociation is expected to have a more favorable pre-exponential factor, however, and should increase in importance with increasing temperature. A second, indirect pathway to phenyl + CH₂O is provided by initial rearrangement of benzoxyl to a bicyclic intermediate (1-oxaspiro[2.5]octa-4,7-dien-5-yl), ring-opening to the phenoxymethyl radical, followed by C–O bond dissociation to the final products (Figure 5). The initial rearrangement steps require only 19.0 kcal mol⁻¹ in

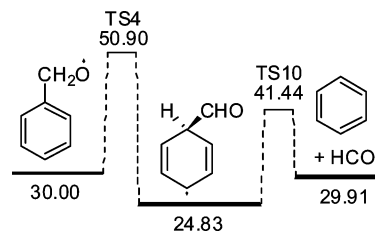


Figure 6. Decomposition of benzoxyl to benzene + HC[•]O via rearrangement to the 2,5-cyclohexadien-4-formyl-1-yl radical.

energy (TS7 and TS8), although pre-exponential factors for these two transition states will be considerably lower than those for the C–C and C–H β -scission reactions. Decomposition of the phenoxymethyl radical requires around 39 kcal mol⁻¹ (TS9) and is expected to be less important than direct dissociation of the benzoxyl radical to phenyl + CH₂O.

Decomposition of the benzoxyl radical to benzene + HC[•]O is also studied, as depicted in Figure 6. In this reaction, the 2,5-cyclohexadien-4-formyl-1-yl radical loses the formyl radical in a low-energy C–C bond β -scission (TS10). The reaction barrier for this dissociation is 16.6 kcal mol⁻¹ (only 11.4 kcal mol⁻¹ above benzoxyl), and the reaction rate should be controlled by the initial intramolecular hydrogen shift. This process is expected to be of some importance, as the barrier is competitive with those for both C–H and C–C β -scission in benzoxyl (Figures 1 and 4, respectively), this process is expected to be of some importance. We note that dissociation of excited 2,5-cyclohexadien-4-formyl-1-yl radicals formed in the benzaldehyde + H association reaction may provide a significant source of benzene in the combustion of alkylated aromatic hydrocarbons, where benzaldehyde is a common intermediate. Benzene is known to be a primary decomposition product of toluene, particularly at lower temperatures, while benzyl formation dominates at higher temperatures.³⁰

Thermochemistry. Thermochemical properties ($\Delta_f H^\circ_{298}$, S°_{298} , $C_p(T)$) for all minima and transition states are listed in Table 1 (transition-state numbering is defined in Figures 1–6). The benzoxyl heat of formation, which we calculate to be 30.0 kcal mol⁻¹, has been previously measured as 29.9 kcal mol⁻¹,³¹ using photoionization mass spectrometry, in good agreement with our calculations. This value has been calculated previously with the G3B3 theoretical method as 31.1 kcal mol⁻¹.¹⁷ In these same studies, the α -hydroxybenzyl radical heat of formation was measured as 6.7 kcal mol⁻¹³¹ and calculated as 11.1 kcal mol⁻¹,¹⁷ compared to our value of 10.00 kcal mol⁻¹. We are not aware of prior experimental or theoretical $\Delta_f H^\circ_{298}$ values for any of the remaining C₇H₇O isomers. The benzene heat of formation is calculated here as 20.44 kcal mol⁻¹, compared to an experimental value of 19.7 kcal mol⁻¹.³² The calculated phenyl radical heat of formation is 82.38 kcal mol⁻¹, giving a benzene C–H BDE of 114.0 kcal mol⁻¹. This BDE is conventionally thought to be 112.9 kcal mol⁻¹,³³ consistent with a phenyl radical heat of formation of 80.5 kcal mol⁻¹.³⁴ The benzaldehyde heat of formation has been measured numerous times, with values ranging from –8.9³⁵ to –7.95 kcal mol⁻¹;³⁶ our calculated enthalpy of –9.51 kcal mol⁻¹ agrees best with values at the lower end of this range. For formaldehyde, enthalpy values of –26.0^{37,38} and –27.7 kcal mol⁻¹²⁴ are often quoted, whereas our calculated value is –26.86 kcal mol⁻¹. A recent theoretical analysis, using isodesmic work reactions, suggested that the formaldehyde heat of formation lies between –26.2 and –26.7 kcal mol⁻¹,³⁷ which is supported by our present result. The formyl radical (HC[•]O) heat of formation has been experi-

TABLE 1: Heats of Formation ($\Delta_f H^\circ_{298}$ kcal mol⁻¹), Entropies (S°_{298} , cal mol⁻¹ K⁻¹), and Heat Capacities (C_p , cal mol⁻¹ K⁻¹) for Species and Intermediates Involved in Benzoxyl Decomposition

	$\Delta_f H^\circ_{298}$	S°_{298}	C_p							
			300 K	400 K	500 K	600 K	800 K	1000 K	1500 K	2000 K
benzoxyl	30.00	84.346	28.155	36.528	43.689	49.508	58.104	64.068	72.823	77.154
α -hydroxybenzyl	10.00	84.198	29.467	38.075	45.180	50.799	58.893	64.453	72.758	77.006
1-oxaspiro[2.5]octa-4,7-dien-5-yl	39.82	80.928	28.102	37.048	44.492	50.420	59.028	64.948	73.669	78.025
phenoxymethyl	30.12	84.510	29.583	38.047	45.036	50.570	58.561	64.053	72.212	76.339
2,5-cyclohexadien-4-formyl-1-yl	24.83	86.514	28.861	37.431	44.585	50.302	58.654	64.436	72.973	77.229
benzaldehyde	-9.51	79.030	26.042	34.048	40.952	46.602	54.965	60.701	68.818	72.612
phenyl	82.38	70.242	18.946	25.510	31.062	35.510	41.974	46.403	52.890	56.116
benzene	20.44	69.082	19.351	26.496	32.616	37.561	44.828	49.874	57.363	61.124
CH ₂ O	-26.86	53.626	8.413	9.258	10.284	11.315	13.147	14.592	16.848	17.980
HC ^o O	9.47	53.634	8.238	8.651	9.135	9.635	10.561	11.306	12.451	13.009
TS1	47.60	83.410	29.193	37.616	44.752	50.531	58.981	64.700	72.724	76.488
TS2	57.75	81.906	27.665	36.258	43.532	49.406	58.005	63.857	72.154	76.097
TS3	47.96	83.549	29.292	37.789	44.910	50.587	58.747	64.241	72.126	75.984
TS4	50.90	81.015	27.086	35.754	43.169	49.166	57.904	63.841	72.366	76.520
TS5	49.88	82.757	29.222	37.673	44.788	50.537	58.961	64.692	72.767	76.546
TS6	60.49	89.625	28.208	35.828	42.499	48.010	56.293	62.130	70.804	75.132
TS7	40.86	79.859	26.544	35.141	42.443	48.327	56.941	62.892	71.658	76.029
TS8	48.95	80.339	27.571	36.211	43.390	49.111	57.442	63.206	71.764	76.072
TS9	68.84	90.632	28.609	36.211	42.860	48.334	56.530	62.297	70.881	75.174
TS10	41.44	87.245	28.729	36.800	43.558	48.991	57.014	62.637	71.033	75.256

mentally determined as 10.1 kcal mol⁻¹,³⁴ in close agreement with our calculated value of 9.47 kcal mol⁻¹.

From the above analysis, we see that the only calculated G3X heat of formation in significant disagreement with experiment is that of the phenyl radical (82.38 kcal mol⁻¹). This phenyl radical heat of formation implies a benzene C–H BDE of 114 kcal mol⁻¹. For a long time, the benzene C–H BDE was considered to be 110–111 kcal mol⁻¹, whereas the currently accepted value is around 113 kcal mol⁻¹. There is some theoretical and experimental evidence, however, in support of an even higher benzene C–H BDE. Nicolaides et al.³⁹ studied the phenyl radical using ab initio methods and determined the heat of formation to be 81.3 kcal mol⁻¹, with a benzene C–H BDE of 113.8 kcal mol⁻¹. Recent G3X calculations using isodesmic work reactions determined the C–H BDEs in toluene to be around 115 kcal mol⁻¹.⁷ If we use a similar work reaction for benzene (C₆H₆ + C₂H₃ → C₆H₅ + C₂H₄), with an ethene C–H BDE of 110.7 kcal mol⁻¹,³³ then we obtain a benzene C–H BDE of 114.7 kcal mol⁻¹. Assuming that the benzene heat of formation is 19.7 kcal mol⁻¹, these isodesmic calculations provide a phenyl radical heat of formation of 82.3 kcal mol⁻¹, in good agreement with the atomization calculations. Experimentally, the benzene C–H bond energy has been measured using negative ion photoelectron spectroscopy, and at 300 K it was assigned to be 113.5 ± 0.5 kcal mol⁻¹ (with phenyl radical heat of formation of 81.2 ± 0.6 kcal mol⁻¹).⁴⁰ On the basis of our results, we feel that it is likely that the actual value of the benzene C–H BDE falls somewhere in the range of 113.5–114.5 kcal mol⁻¹, consistent with recent theory and experiment.

Transition States and Elementary Reaction Rates. Transition states were located for each of the proposed elementary reaction steps and are depicted in Figure 7. High-pressure limit rate constants for these reactions were calculated between 300 and 2000 K and fit to the rate parameters E_a , A' , and n (listed in Table 2).

Reaction Kinetics. The kinetics of benzoxyl decomposition was studied for temperatures from 300 to 2000 K and for pressures from 0.01 to 100 atm, with RRKM theory. The total rate constant for benzoxyl decomposition is plotted in Figure 8, as a function of temperature and pressure. Here we find that,

for pressures of around 1 atm and below, falloff plays a significant role at even moderate temperatures (ca. 1000 K). This decomposition reaction is fast, even at low temperatures, with a half-life of 10 μ s at 500 K; during combustion it is therefore unlikely that the benzoxyl will exist long enough to participate in bimolecular reactions.

Rate constants for the six individual reaction pathways at 1 atm are plotted in Figure 9, with branching ratios to the three different product sets shown in Figure 10. From Figure 10 we discover that, at atmospheric pressure, benzaldehyde is the dominant benzoxyl decomposition product for all temperatures considered. At low temperatures (<1000 K), benzaldehyde formation corresponds to more than 80% of the total reaction, but this decreases to around 50% at high temperatures (2000 K); it is therefore important that decomposition reactions to products other than benzaldehyde be included in kinetic models. Figure 9 reveals that the direct mechanism is the major source of benzaldehyde + H, with a small fraction produced via the 2,5-cyclohexadien-4-formyl-1-yl radical in the “indirect II” mechanism. The “indirect I” mechanism, where benzoxyl isomerizes to the α -hydroxybenzyl radical, is unimportant at all temperature and pressure conditions because of the large barrier to formation of the radical intermediate. Our RRKM calculations do indicate, however, that once formed the α -hydroxybenzyl radical proceeds almost exclusively to benzaldehyde + H, with little reverse reaction to benzoxyl. Accordingly, α -hydroxybenzyl formed via other reaction pathways is expected to principally dissociate to benzaldehyde + H.

Formation of benzene + HC^oO is the second most important channel in decomposition of the benzoxyl radical at temperatures up to 1600 K. At 1000 K, this product set constitutes around 10% of the reaction products, increasing to around 20% at 2000 K. The phenyl + CH₂O product set is relatively unimportant at low temperatures but increases in significance with temperature, accounting for around 30% of the decomposition products at 2000 K. The direct channel is the main source of phenyl + CH₂O at most temperatures considered, with the indirect mechanism, proceeding via the phenoxymethyl radical, dominating at high temperatures.

The above results indicate that benzene + HC^oO and phenyl + CH₂O should be included as products of benzoxyl radical

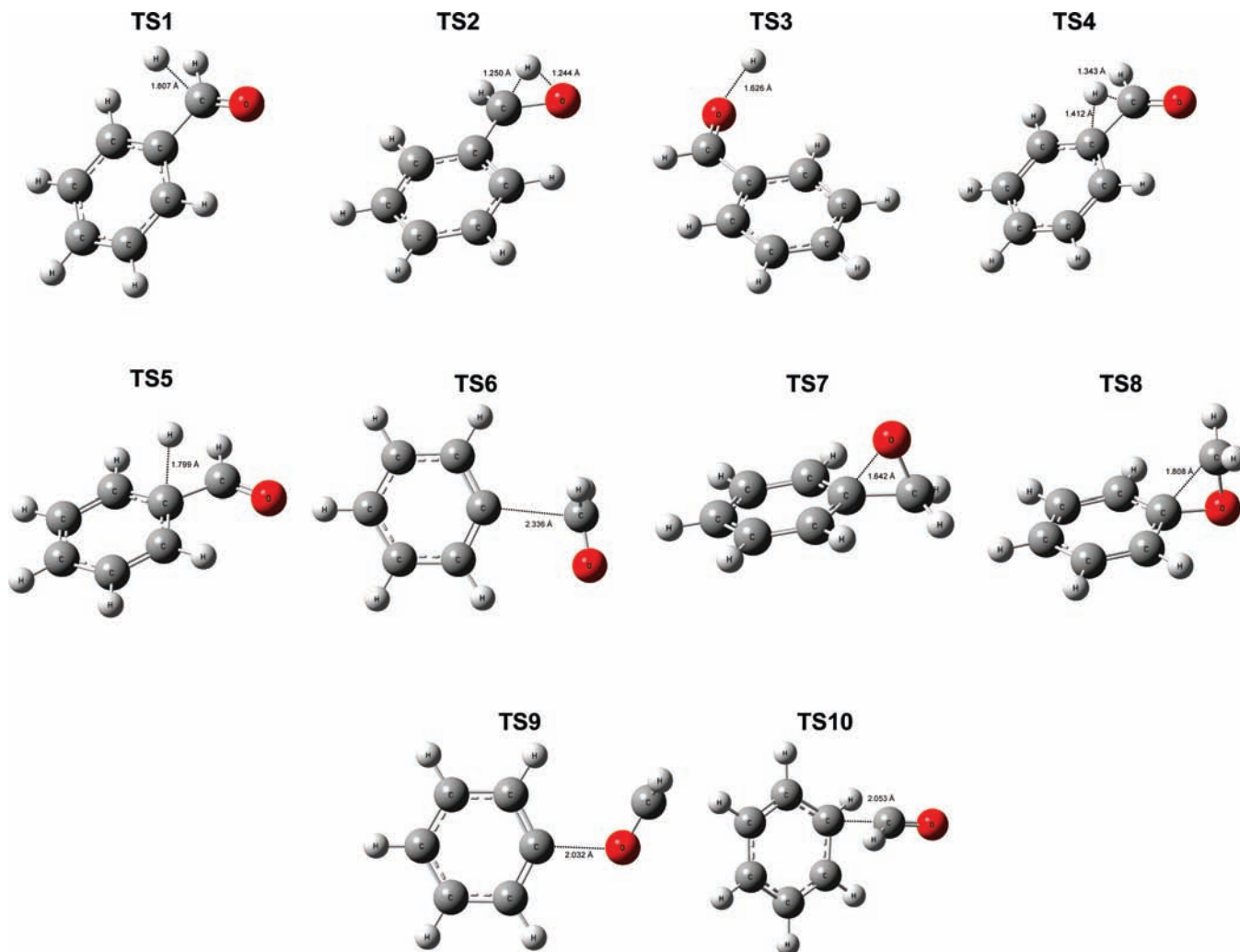


Figure 7. Optimized geometries of transition-state structures in the proposed benzoxyl decomposition mechanism, at the B3LYP/6-31G(2df,p) level.

TABLE 2: Elementary Rate Parameters (E_a , A' , n) for Forward (f) and Reverse (r) Reactions in the Proposed Benzoxyl Decomposition Mechanisms^a

	A' (f)	n (f)	E_a (f)	A' (r)	n (r)	E_a (r)
benzoxyl \rightarrow benzaldehyde + H (TS1)	5.07×10^8	1.560	16.85	3.28×10^{-16}	1.670	4.65
benzoxyl \rightarrow α -hydroxybenzyl (TS2)	1.82×10^{-2}	4.261	19.86	2.06×10^{-1}	3.878	39.96
α -hydroxybenzyl \rightarrow benzaldehyde + H (TS3)	1.26×10^9	1.278	36.83	7.21×10^{-17}	1.770	4.53
benzoxyl \rightarrow 2,5-cyclohexadien-4-formyl-1-yl (TS4)	1.67×10^8	1.426	19.26	3.16×10^{-8}	1.153	24.54
2,5-cyclohexadien-4-formyl-1-yl \rightarrow benzaldehyde + H (TS5)	2.67×10^7	1.602	23.55	9.10×10^{-18}	1.984	6.07
benzoxyl \rightarrow phenyl + CH ₂ O (TS6)	1.09×10^{14}	0.157	31.16	2.00×10^{-21}	2.572	4.63
benzoxyl \rightarrow 1-oxaspiro[2.5]octa-4,7-dien-5-yl (TS7)	1.17×10^{11}	0.398	11.17	1.27×10^{13}	-0.031	1.68
1-oxaspiro[2.5]octa-4,7-dien-5-yl \rightarrow phenoxymethyl (TS8)	3.16×10^{12}	0.233	9.71	8.78×10^{10}	0.442	19.03
phenoxymethyl \rightarrow phenyl + CH ₂ O (TS9)	2.61×10^{14}	0.054	39.28	1.59×10^{-21}	2.689	12.93
2,5-cyclohexadien-4-formyl-1-yl \rightarrow benzene + HC \cdot O (TS10)	6.72×10^{12}	0.229	17.22	2.65×10^{-22}	2.788	11.07

^a $k^\infty = A'T^n \exp(-E_a/RT)$. Units: kcal mol⁻¹, s⁻¹, cm³ molecule⁻¹ s⁻¹.

decomposition, in addition to the commonly considered products benzaldehyde + H. Input rate parameters (E_a , A' , n) for formation of these three products at 1 atm are listed in Table 3 (values at other pressures are available in the Supporting Information). The introduction of these reactions into kinetic models should lead to improved modeling of aromatic combustion.

Calculated barrier heights are expected to be accurate to within 1.5 kcal mol⁻¹. To investigate the effect of this uncertainty, the overall rate expressions for benzoxyl decomposition to different product sets at 1 atm (reported in Table 3) were plotted with $E_a \pm 1.5$ kcal mol⁻¹ (Figure 11). At

temperatures below around 1000 K, where the barrier height uncertainty has the largest effect on k , our calculations appear to be able to resolve the ordering of the three different product sets. At higher temperatures, it is difficult to distinguish between the two minor product channels, but decomposition to benzaldehyde + H is predicted to remain dominant up to around 1600 K, even considering a net change of 3 kcal mol⁻¹ in the relative barrier heights. At temperatures approaching 2000 K, it becomes difficult to discriminate between any of the three product sets. At such high temperatures, the decomposition kinetics is influenced significantly by falloff effects, making differences in the barrier heights less important.

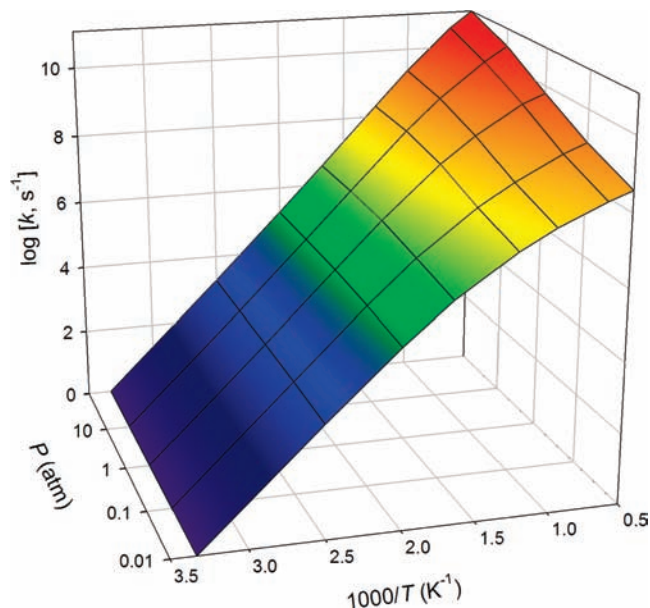


Figure 8. Total rate constants for decomposition of the benzoyl radical, as a function of temperature and pressure.

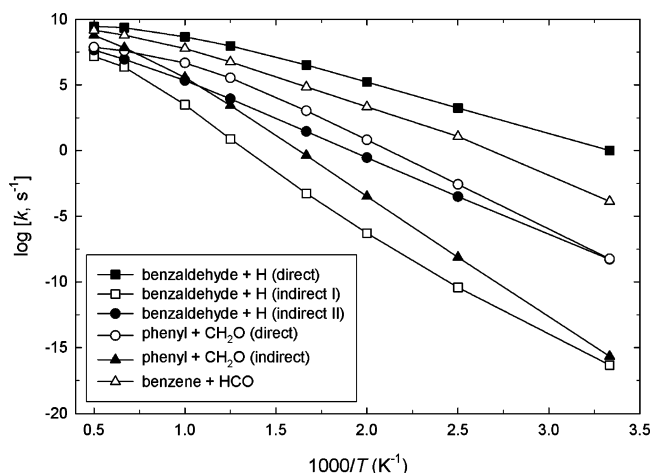


Figure 9. Rate constants for benzyl decomposition to benzaldehyde + H, phenyl + CH₂O, and benzene + HC'O, at 1 atm.

To establish how sensitive our results are to collisional energy transfer and falloff, we investigated the effect of $\langle \Delta E_{\text{down}} \rangle$ on the kinetics of benzoyl radical decomposition. In recent studies, we found that relatively large values of $\langle \Delta E_{\text{down}} \rangle$, on the order of 2000 cm⁻¹, were required to reproduce falloff effects in experimental results for thermal decomposition reactions.^{7,29} This may be related to the presence, in practice, of more efficient colliders than N₂, increasing the apparent value of $\langle \Delta E_{\text{down}} \rangle$. Alternatively, our results could be explained by a temperature-dependent model for $\langle \Delta E_{\text{down}} \rangle$, where the temperature dependence is still a matter of considerable uncertainty.⁴¹ Apparent rate constants were determined for each of the reaction channels in benzoyl decomposition (excluding the benzaldehyde + H “indirect I” reaction, which is of negligible importance), between 600 and 2000 K and at 1 atm, using $\langle \Delta E_{\text{down}} \rangle$ values of 500, 1000, 2000, and 3000 cm⁻¹. Overall rate constants to the three different product sets are plotted in Figure 12. The choice of $\langle \Delta E_{\text{down}} \rangle$ has a large effect on the predicted decomposition rate, with rate constants varying by over an order of magnitude at temperatures of around 1000 K and above. The branching ratios between the different products are relatively unaffected, however. At 2000 K, branching fractions vary from 0.49 to 0.55

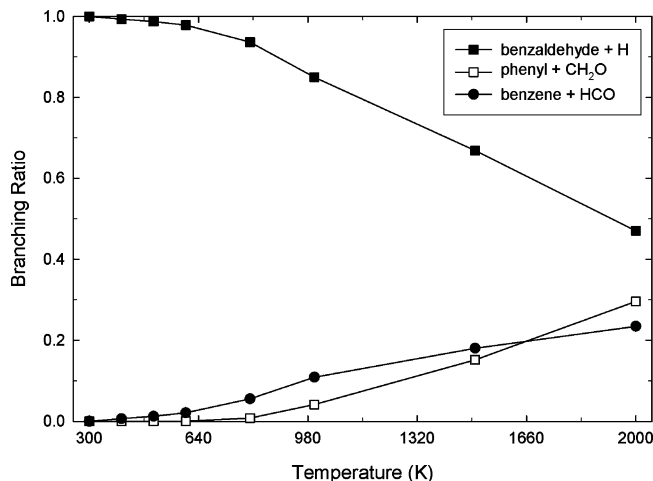


Figure 10. Branching ratios to benzaldehyde + H, phenyl + CH₂O, and benzene + HC'O product sets in benzoyl decomposition, at 1 atm.

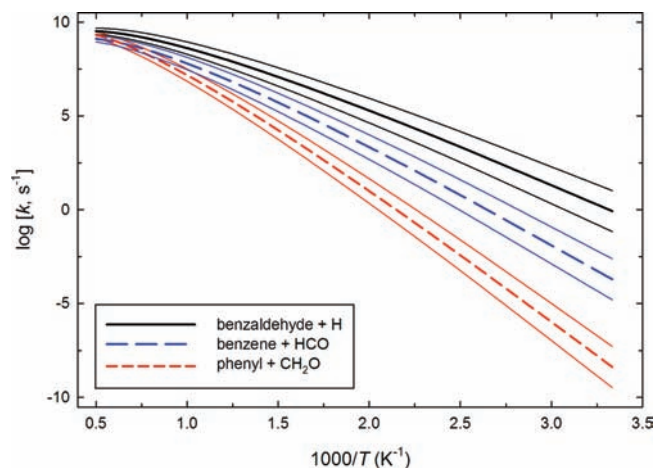


Figure 11. Calculated rate expressions for benzoyl decomposition to different product sets, with associated uncertainties (faint lines).

TABLE 3: Apparent Rate Parameters (E_a , A' , n) for Benzoyl Decomposition at 1 atm^a

	A' (s ⁻¹)	n	E_a (kcal mol ⁻¹)
benzoyl → benzaldehyde + H	5.26×10^{28}	-5.081	22.25
benzoyl → phenyl + CH ₂ O	7.21×10^{33}	-6.210	36.85
benzoyl → benzene + HC'O	2.37×10^{32}	-6.095	28.81

$$^a k = A'T^n \exp(-E_a/RT).$$

for benzaldehyde + H, 0.20 to 0.24 for benzene + HC'O, and 0.25 to 0.28 for phenyl + CH₂O.

Comparison with Current Kinetic Models. Prior kinetic models for the oxidation of toluene (and other substituted aromatic hydrocarbons) treat benzoyl decomposition in a variety of ways. Some studies assume that the benzyl + HO₂ reaction (the main source of benzoyl) proceeds directly to benzaldehyde + OH + H, and in some instances also to phenyl + OH + CH₂O. For example, Emdee et al.⁴² estimated a rate constant of 2.5×10^{14} cm³ mol⁻¹ s⁻¹ for the benzyl + HO₂ → benzaldehyde + OH + H reaction, and 8.0×10^{13} cm³ mol⁻¹ s⁻¹ for the benzyl + HO₂ → phenyl + OH + CH₂O reaction (later updated to 3.67×10^{14} and 1.17×10^{14} cm³ mol⁻¹ s⁻¹, respectively).^{2,4} These rate constants yield a branching ratio of 0.76 for the benzaldehyde product channel and 0.24 for the phenyl channel. Other studies treat the benzyl + HO₂ reaction as forming benzoyl + OH, followed by unimolecular (and in

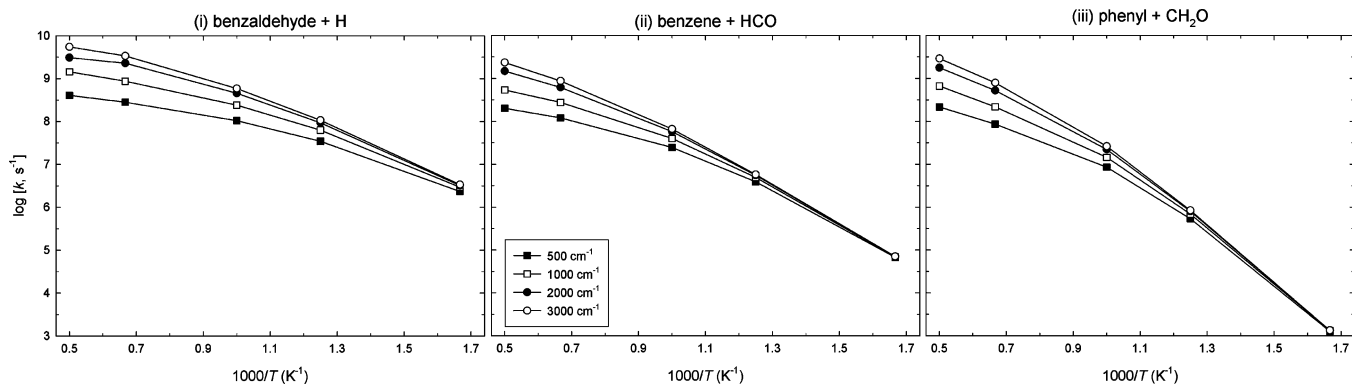


Figure 12. Effect of $\langle \Delta E_{\text{down}} \rangle$ on calculated rate constants for benzoxyl decomposition to benzaldehyde + H, benzene + HCO, and phenyl + CH₂O.

some cases bimolecular) reactions of the benzoxyl radical. Brezinsky et al.¹⁸ used $k = 1.3 \times 10^{14} \exp(-554/T)$ for benzoxyl radical decomposition to benzaldehyde + H, far exceeding our calculated rate constants. Andrae et al.⁶ incorporated this rate constant into their model for toluene oxidation and added the estimate $k = 4.0 \times 10^{13} \exp(-1007/T)$ for decomposition to phenyl + CH₂O (again, much greater than our calculated value). The Andrae et al.⁶ rate constants result in a branching ratio to phenyl + CH₂O of 0.06 at 300 K and 0.20 at 2000 K, in fair agreement with our findings. Bounaceur et al.³ treated benzoxyl decomposition with a similar mechanism but used estimated rate constants of $2.0 \times 10^{13} \exp(-13840/T)$ for both the benzaldehyde + H and phenyl + CH₂O product sets. This study appears to overestimate the branching ratio to phenyl + CH₂O; the rate constant for decomposition to phenyl + CH₂O is in quite good agreement with that calculated here, but the benzaldehyde + H rate constant is drastically underestimated. Bounaceur et al.³ also included in their mechanism a decomposition reaction for the α -hydroxybenzyl radical (to benzaldehyde + H), which is formed by hydrogen abstraction reactions in benzyl alcohol. The rate constant for α -hydroxybenzyl decomposition was estimated as $k = 2.0 \times 10^{14} \exp(-11730/T)$. Assuming that the α -hydroxybenzyl radical decomposes only to benzaldehyde + H via O–H bond scission (i.e., TS3 in Figure 2), then we calculate a high-pressure limit rate constant $k = 5.75 \times 10^5 T^{2.208} \exp(-17036/T)$; this is at least several orders of magnitude slower than the Bounaceur et al.³ estimate, with both a smaller pre-exponential factor and a larger activation energy.

Figure 13 compares our rate expression for decomposition of benzoxyl to benzaldehyde + H (at 1 atm) with those used in the kinetic models of Brezinsky et al.¹⁸ and Bounaceur et al.³ The expression reported here provides rate constants intermediate between those of the two previous studies (except at very high temperatures, due to falloff), with closest agreement to the Bounaceur et al.³ expression. In Figure 14, our calculated expression for the benzoxyl \rightarrow phenyl + CH₂O rate constant is plotted and compared to those from Andrae et al.⁶ and Bounaceur et al.³ Agreement between our calculated values and the Bounaceur et al.³ estimate is good, while the Andrae et al.⁶ rate constants are many orders of magnitude too large, particularly at lower temperatures. It is important to emphasize, however, that in this instance branching ratios to different products are the critical property that needs to be reproduced by the rate expressions. Since benzoxyl is short-lived, the magnitude of the decomposition rate constants may not be that important (as long as they are not too small). For example, while the rate constant expressions in refs 18 and 6 significantly

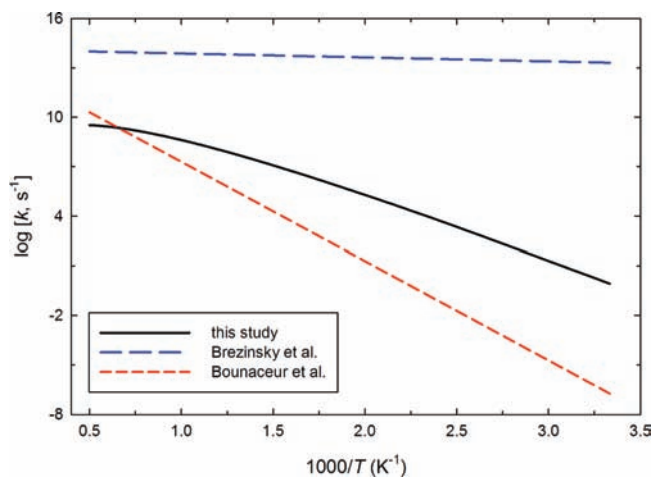


Figure 13. Rate expressions for decomposition of benzoxyl to benzaldehyde + H. Comparison of theoretical prediction with current kinetic models.

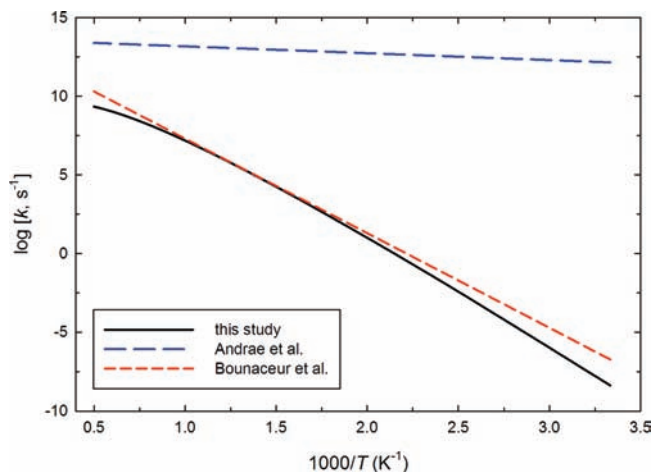


Figure 14. Rate expressions for decomposition of benzoxyl to phenyl + CH₂O. Comparison of theoretical prediction with current kinetic models.

overestimate the rate of benzoxyl decomposition, the branching ratios to benzaldehyde + H and phenyl + CH₂O appear to be relatively accurate at relevant combustion temperatures.

Conclusions

Decomposition of the benzoxyl radical has been studied using computational chemistry and RRKM rate theory. Decomposition pathways to benzaldehyde + H, the phenyl radical + formal-

dehyde (CH₂O), and benzene + the formyl radical (HC[•]O) are considered. The benzene pathway is a stepwise process and proceeds with a barrier of only 20.9 kcal mol⁻¹, which is competitive with direct C–H and C–C bond scission reactions in benzoxyl. RRKM simulations of the benzoxyl decomposition mechanism reveal that, while benzaldehyde + H are the main products, the benzene and phenyl pathways are also of importance and should be included in detailed kinetic models of aromatic combustion.

Acknowledgment. Partial funding was provided by the U.S. Air Force Phase II STTR program (Contract No. FA8650-06-C-2658).

Supporting Information Available: Geometries (in Cartesian coordinates) and energies (in hartrees) for all stationary points, internal rotor potentials, and input rate parameters (E_a , A' , n) for kinetic modeling of benzoxyl decomposition from 0.01 to 100 atm. This material is available free of charge via the Internet at <http://pubs.acs.org>.

References and Notes

- (1) Roubaud, A.; Minetti, R.; Sochet, L. R. *Combust. Flame* **2000**, *121*, 535.
- (2) Sivaramakrishnan, R.; Tranter, R. S.; Brezinsky, K. *Combust. Flame* **2004**, *139*, 340.
- (3) Bounaceur, R.; Da Costa, I.; Fournet, R.; Billaud, F.; Battin-Leclerc, F. *Int. J. Chem. Kinet.* **2005**, *37*, 25.
- (4) Sivaramakrishnan, R.; Tranter, R. S.; Brezinsky, K. *Proc. Combust. Inst.* **2005**, *30*, 1165.
- (5) Battin-Leclerc, F.; Bounaceur, R.; Belmekki, N.; Glaude, P. A. *Int. J. Chem. Kinet.* **2006**, *38*, 284.
- (6) Andrae, J.; Björnbohm, P.; Cracknell, R. F.; Kalghatgi, G. *Combust. Flame* **2007**, *149*, 2.
- (7) da Silva, G.; Cole, J. A.; Bozzelli, J. W. *J. Phys. Chem. A* **2009**, *113*, 6111.
- (8) Murakami, Y.; Oguchi, T.; Hashimoto, K.; Nosaka, Y. *J. Phys. Chem. A* **2007**, *111*, 13200.
- (9) Uc, V. H.; Alvarez-Idaboy, J. R.; Galano, A.; García-Cruz, I.; Vivier-Bunge, A. *J. Phys. Chem. A* **2006**, *110*, 10155.
- (10) Oehlschlaeger, M. A.; Davidson, D. F.; Hanson, R. K. *Combust. Flame* **2006**, *147*, 195.
- (11) da Silva, G.; Chen, C.-C.; Bozzelli, J. W. *J. Phys. Chem. A* **2007**, *111*, 8663.
- (12) Carpenter, B. K. *J. Am. Chem. Soc.* **1993**, *115*, 9806.
- (13) Mebel, A. M.; Lin, M. C. *J. Am. Chem. Soc.* **1994**, *116*, 9577.
- (14) Barckholtz, C.; Fadden, M. J.; Hadad, C. M. *J. Phys. Chem. A* **1999**, *103*, 8108.
- (15) da Silva, G.; Bozzelli, J. W. *J. Phys. Chem. A* **2008**, *112*, 3566.
- (16) Hippler, H.; Reihs, C.; Troe, J. *Proc. Combust. Inst.* **1990**, *23*, 37.
- (17) da Silva, G.; Bozzelli, J. W. *Proc. Combust. Inst.* **2009**, *32*, 287.
- (18) Brezinsky, K.; Litzinger, T. A.; Glassman, I. *Int. J. Chem. Kinet.* **1984**, *16*, 1053.
- (19) Bartels, M.; Edelbuttel-Einhaus, J.; Hoyermann, K. *Proc. Combust. Inst.* **1989**, *22*, 1041.
- (20) Hermans, I.; Peeters, J.; Vereecken, L.; Jacobs, P. A. *ChemPhys-Chem* **2007**, *8*, 2678.
- (21) Dagaut, P.; Pengloan, G.; Ristori, A. *Phys. Chem. Chem. Phys.* **2002**, *4*, 1846.
- (22) Chenoweth, K.; van Duin, A. C. T.; Goddard, W. A., III. *J. Phys. Chem. A* **2008**, *112*, 1040.
- (23) Curtiss, L. A.; Redfern, P. C.; Raghavachari, K.; Pople, J. A. *J. Chem. Phys.* **2001**, *114*, 108.
- (24) Chase, M. W., Jr. *J. Phys. Chem. Ref. Data* **1998**, *1*.
- (25) Frisch, M. J.; Trucks, G. W.; Schlegel, H. B.; Scuseria, G. E.; Robb, M. A.; Cheeseman, J. R.; Montgomery, J. A., Jr.; Vreven, T.; Kudin, K. N.; Burant, J. C.; Millam, J. M.; Iyengar, S. S.; Tomasi, J.; Barone, V.; Mennucci, B.; Cossi, M.; Scalmani, G.; Rega, N.; Petersson, G. A.; Nakatsuji, H.; Hada, M.; Ehara, M.; Toyota, K.; Fukuda, R.; Hasegawa, J.; Ishida, M.; Nakajima, T.; Honda, Y.; Kitao, O.; Nakai, H.; Klene, M.; Li, X.; Knox, J. E.; Hratchian, H. P.; Cross, J. B.; Bakken, V.; Adamo, C.; Jaramillo, J.; Gomperts, R.; Stratmann, R. E.; Yazyev, O.; Austin, A. J.; Cammi, R.; Pomelli, C.; Ochterski, J. W.; Ayala, P. Y.; Morokuma, K.; Voth, G. A.; Salvador, P.; Dannenberg, J. J.; Zakrzewski, V. G.; Dapprich, S.; Daniels, A. D.; Strain, M. C.; Farkas, O.; Malick, D. K.; Rabuck, A. D.; Raghavachari, K.; Foresman, J. B.; Ortiz, J. V.; Cui, Q.; Baboul, A. G.; Clifford, S.; Cioslowski, J.; Stefanov, B. B.; Liu, G.; Liashenko, A.; Piskorz, P.; Komaromi, I.; Martin, R. L.; Fox, D. J.; Keith, T.; Al-Laham, M. A.; Peng, C. Y.; Nanayakkara, A.; Challacombe, M.; Gill, P. M. W.; Johnson, B.; Chen, W.; Wong, M. W.; Gonzalez, C.; Pople, J. A. *Gaussian 03*, revision D.01; Gaussian, Inc.: Wallingford, CT, 2004.
- (26) Zheng, J.; Zhao, Y.; Truhlar, D. G. *J. Chem. Theory Comput.* **2009**, *5*, 808.
- (27) Mokrushin, V.; Bedanov, V.; Tsang, W.; Zachariah, M.; Knyazev, V. *ChemRate*, version 1.5.2; National Institute of Standards and Technology: Gaithersburg, MD, 2006.
- (28) Eckart, C. *Phys. Rev.* **1930**, *35*, 1303.
- (29) da Silva, G. *Chem. Phys. Lett.* **2009**, *474*, 13.
- (30) Li, Y.; Zhang, L.; Tian, Z.; Yuan, T.; Wang, J.; Yang, B.; Qi, F. *Energy Fuels* **2009**, *23*, 1473.
- (31) Ponomarev, D. A.; Takhistov, V. V.; Orlov, V. M. *Zh. Obshch. Khim.* **1996**, *66*, 1821.
- (32) Cioslowski, J.; Schimeczek, M.; Liu, G.; Stoyanov, V. *J. Chem. Phys.* **2000**, *113*, 9377.
- (33) Blanksby, S. J.; Ellison, G. B. *Acc. Chem. Res.* **2003**, *36*, 255.
- (34) Ervin, K. M.; DeTuri, V. F. *J. Phys. Chem. A* **2002**, *106*, 9947.
- (35) Solly, R. K.; Benson, S. W. *J. Chem. Thermodyn.* **1971**, *3*, 203.
- (36) Kudchadker, S. A.; Kudchadker, A. P. *Ber. Bunsen-Ges. Phys. Chem.* **1975**, *12*, 432.
- (37) da Silva, G.; Bozzelli, J. W.; Sebbar, N.; Bockhorn, H. *Chem-PhysChem* **2006**, *7*, 1119.
- (38) Cox, J. D.; Pilcher, G. *Thermochemistry of Organic and Organometallic Compounds*; Academic Press: New York, 1970.
- (39) Nicolaidis, A.; Smith, D. M.; Jensen, F.; Radom, L. *J. Am. Chem. Soc.* **1997**, *119*, 8083.
- (40) Davico, G. E.; Bierbaum, V. M.; DePuy, C. H.; Ellison, G. B.; Squires, R. R. *J. Am. Chem. Soc.* **1995**, *117*, 2590.
- (41) Oref, I.; Tardy, D. C. *Chem. Rev.* **1990**, *90*, 1407.
- (42) Emdee, J. L.; Brezinsky, K.; Glassman, I. *J. Phys. Chem.* **1992**, *96*, 2151.

JP902458D